ACS NANO
Cite This: ACS Nano 2019, 13, 2936–2947
www.acsnano.org

ARTICLE

Biomimetic Glyconanoparticle Vaccine for Cancer Immunotherapy

Eliran Moshe Reuven,[†,#] Shani Leviatan Ben-Arye,[†,#] Hai Yu,[‡] Roberto Duchi,[§] Andrea Perota,[§] Sophie Conchon,[∥] Shirley Bachar Abramovitch,[†] Jean-Paul Soulillou,[∥] Cesare Galli,[§,⊥] Xi Chen,[‡] and Vered Padler-Karavani*[,†]

[†]Department of Cell Research and Immunology, The George S. Wise Faculty of Life Sciences, Tel Aviv University, Tel Aviv 69978, Israel

[‡]Department of Chemistry, University of California, Davis, California 95616, United States

[§]Avantea, Laboratory of Reproductive Technologies, Via Porcellasco 7/F, 26100 Cremona, Italy

[∥]Institut de Transplantation-Urologie-Néphrologie, INSERM Unité Mixte de Recherche 1064, Centre Hospitalo Universitaire de Nantes, Nantes 44000, France

[⊥]FondazioneAvantea Cremona, Via Cabrini, 12, 26100 Cremona, Italy

Supporting Information

ABSTRACT: **Cancer immunotherapy aims to harness the immune system to combat malignant processes. Transformed cells harbor diverse modifications that lead to formation of neoantigens, including aberrantly expressed cell surface carbohydrates. Targeting tumor-associated carbohydrate antigens (TACA) hold great potential for cancer immunotherapy. *N*-glycolylneuraminic acid (Neu5Gc) is a dietary non-human immunogenic carbohydrate that accumulates on human cancer cells, thereby generating neoantigens. In mice, passive immunotherapy with anti-Neu5Gc antibodies inhibits growth of Neu5Gc-positive tumors. Here, we designed an active cancer vaccine immunotherapy strategy to target Neu5Gc-positive tumors. We generated biomimetic glyconanoparticles using engineered αGal knockout porcine red blood cells to form nanoghosts (NGs) that either express (NG^{pos}) or lack expression (NG^{neg}) of Neu5Gc-glycoconjugates in their natural context. We demonstrated that optimized immunization of "human-like" Neu5Gc-deficient *Cmah*$^{-/-}$ mice with NG^{pos} glyconanoparticles induce a strong, diverse and persistent anti-Neu5Gc IgG immune response. The resulting anti-Neu5Gc IgG antibodies were also detected within Neu5Gc-positive tumors and inhibited tumor growth *in vivo*. Using detailed glycan microarray analysis, we further demonstrate that the kinetics and quality of the immune responses influence the efficacy of the vaccine. These findings reinforce the potential of TACA neoantigens and the dietary non-human sialic acid Neu5Gc, in particular, as immunotherapy targets.**

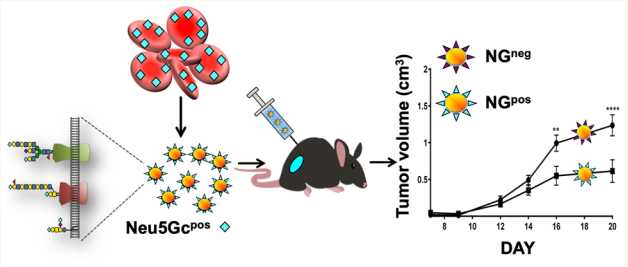

KEYWORDS: *neoantigen, cancer immunotherapy, biomimetic, glyconanoparticle, glycan microarray, sialic acid, N-glycolylneuraminic acid*

Immunotherapy for cancer treatment has made important advancements in recent years.[1,2] It generally aims to induce or expand the host anticancer immune response that can distinguish subtle differences between cancer and normal cells.[3] The three common immunotherapies are targeted cellular therapeutics (i.e., adoptive T cell therapy),[4−6] immune checkpoint blockade (e.g., blocking monoclonal antibodies targeting CTLA-4, PD-1 or PD-L1),[7−9] and therapeutic cancer vaccines.[10] Based on their composition, vaccines can stimulate adaptive immune responses of tumor-specific cytotoxic T cells and antibodies against tumor-associated antigens,[3,11,12] yet with only limited success,[3,11,13−15] mainly due to difficulties in identifying target antigens.[3]

Although carbohydrates have long been considered to be poorly immunogenic, their enormous potential as therapeutic targets led to the design of carbohydrate-based vaccines.[16−19] Carbohydrate chains (glycans) are ubiquitously expressed on the surface of cells, where they are optimally located for recognition by antibodies and immune receptors, either for protection or for elimination. Thus, various carbohydrate-

Received: September 21, 2018
Accepted: March 6, 2019
Published: March 6, 2019

DOI: 10.1021/acsnano.8b07241
ACS Nano 2019, 13, 2936–2947

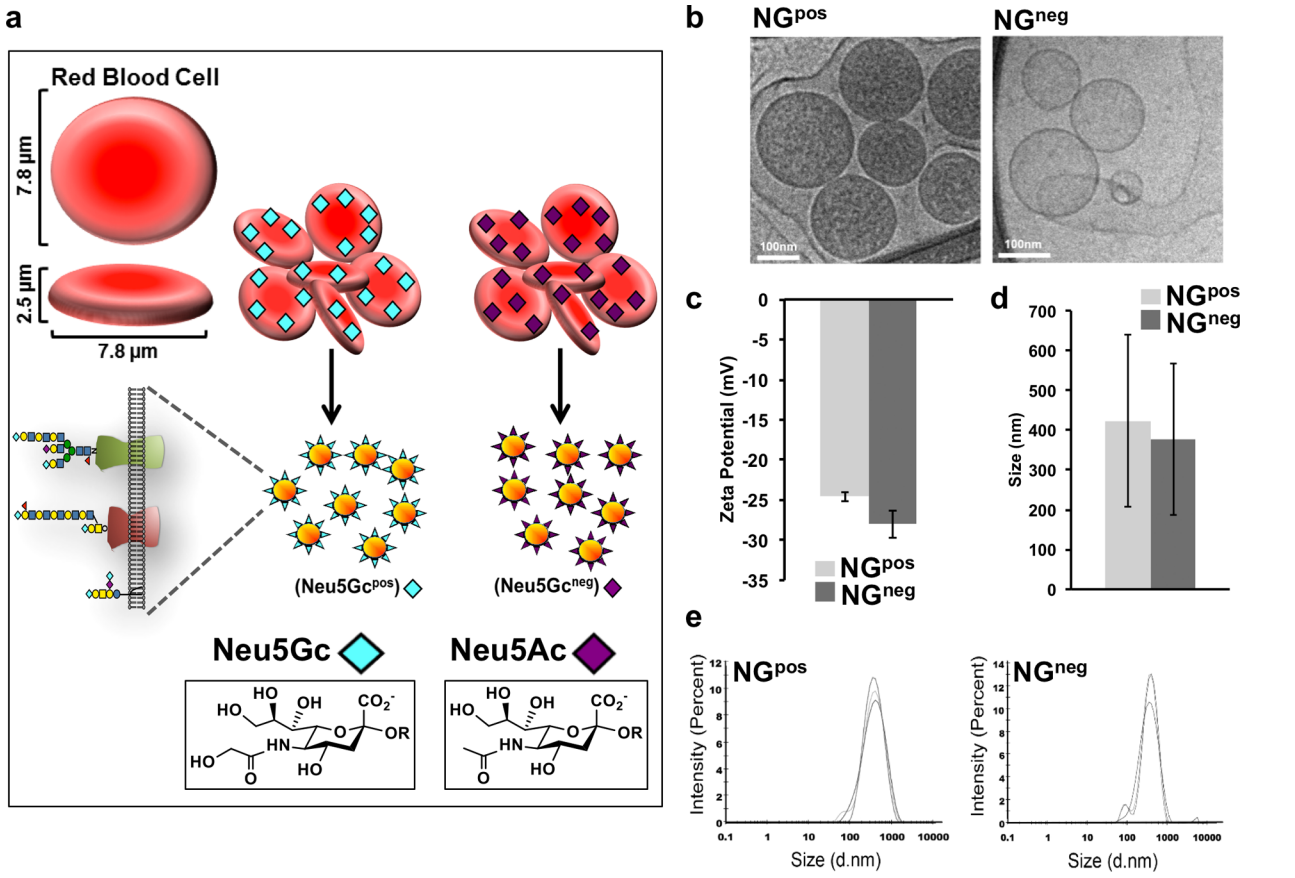

Figure 1. Physiochemical characterization of porcine-derived nanoghosts (NGs). (a) Schematic representation of red blood cells (RBCs) and NGs prepared from RBCs of two porcine strains that express various Sia-containing glycoproteins with either terminal Neu5Gc (αGal-deficient strain; NG^{pos}) or terminal Neu5Ac (Neu5Gc- and αGal-deficient strain; NG^{neg}). (b) Transmission electron micrograph (TEM) analysis of NG^{pos} and NG^{neg}. Freshly prepared NGs were applied onto a plasma-etched carbon grid in CryoPlunge 3 unit (Gatan Instruments) employing a double-blot technique for 2 s and then plunged into liquid ethane and transferred under liquid nitrogen to cryo-TEM (FEI; Tecnai G2). Images were captured using DigitalMicrograph software (Gatan) (representative of two independent experiments). (c) Zeta potential of freshly prepared NGs was measured. (d, e) Size of freshly prepared NGs was measured. NGs were diluted to 20 µg protein/mL (in ddH_2O for zeta potential or PBS pH 7.4 for size) and measured in a Malvern Nano ZS Zetasizer (each experimental result is an average of at least three independent measurements).

based vaccines have been actively pursued to target not only various bacteria, viruses, or parasites but also cancer cells.[16,17,20] Cancer cells express aberrant glycosylation patterns compared to normal cells, and TACAs can be targeted for tumor cell killing through direct apoptosis, Fc-positive effector cells, or complement.[21−23]

Sialic acids (Sia) cover cell-surface glycans and frequently have altered expression on cancer cells that correlates with cancer progression and/or metastasis.[24−28] *N*-acetylneuraminic acid (Neu5Ac) and its hydroxylated form, *N*-glycolylneuraminic acid (Neu5Gc), are the two major Sia forms in mammals.[29] While humans cannot synthesize Neu5Gc due to a specific inactivation of the *CMAH* gene,[30] this non-human Sia incorporates into human cells through consumption of red meat and dairy[31,32] and substantially accumulates on carcinomas.[33] Thus, Neu5Gc presentation on tumor cells generates a variety of neoantigens that could potentially be targeted for immunotherapy. Passive transfer of anti-Neu5Gc antibodies inhibited growth of Neu5Gc-positive tumors *in vivo* in the human-like Neu5Gc-deficient $Cmah^{-/-}$ mouse model.[34,35]

Here, we investigated the potential targeting of Neu5Gc-neoantigens for immunotherapy by an active cancer vaccine. For this purpose, we generated biomimetic glyconanoparticles that express Neu5Gc-glycoconjugates in their natural context. As a control, we also generated equivalent glyconanoparticles that express Neu5Ac-glycoconjugates. Then we optimized immunization of $Cmah^{-/-}$ mice with the cancer vaccine glyconanoparticles to induce a potent and sustained anti-Neu5Gc immune response that inhibited tumor growth *in vivo*. Vaccine response was monitored by a robust high-throughput sialoglycan microarray, and the analysis revealed that the kinetics and quality of the developed immune response influence the efficacy of the therapeutic cancer vaccine.

RESULTS AND DISCUSSION

Generation and Physical Characterization of Biomimetic Glyconanoparticles. We designed an erythrocyte-based active cancer vaccine immunotherapy strategy to target Neu5Gc-positive tumors. Erythrocytes (red blood cells; RBCs) are attractive for various nanobiomedical applications.[36−38] RBCs are biconcave disk-shaped cells (~7.8 µm × ~2.5 µm) that lack a nucleus, with a plasma membrane surface area of ~160 μm^2 (Figure 1A).[39,40] RBCs are resistant to adhesion to the endothelium, partly mediated by their glycocalyx that is abundantly covered with negatively charged sialic acids.[39,41] To

DOI: 10.1021/acsnano.8b07241
ACS Nano 2019, 13, 2936−2947

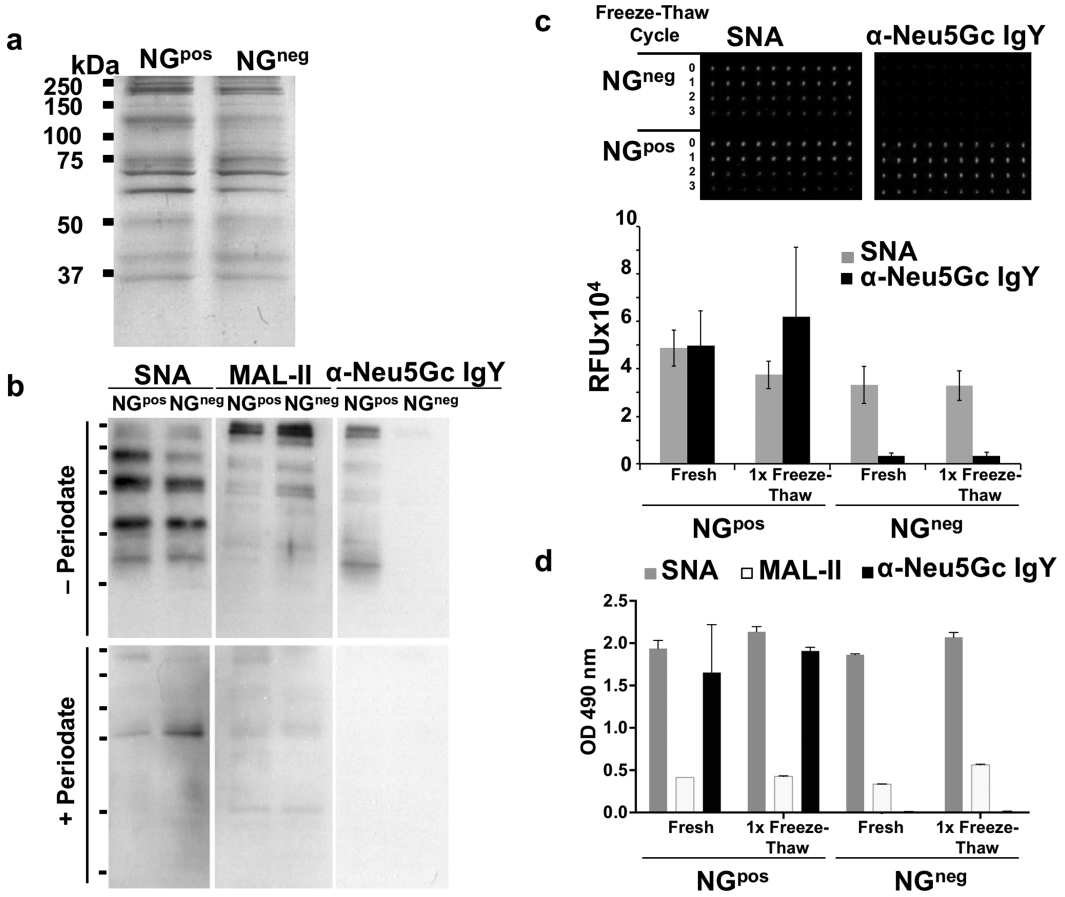

Figure 2. Biochemical characterization of NG^{pos} and NG^{neg}. NGs were diluted in sample buffer to 40 μg protein/mL, loaded 10 μL/lane, then separated on 12% SDS–PAGE gel. (a) Silver staining of freshly prepared NGs revealed similar protein content in both NG^{pos} and NG^{neg}. (b) Sialic acid content of NGs was analyzed by Western blot with the biotinylated lectins Bio-SNA (binds Siaα2–6-linked) and Bio-MAL-II (binds Siaα2–3-linked), detected by HRP-streptavidin; and chicken anti-Neu5Gc IgY was detected by HRP-donkey-anti-chicken IgY. Specificity was analyzed by pretreatment of the blot with mild periodate oxidation (bottom panel; + periodate) that truncates Sia side chain (carbons C-8 and C-9), leading to loss of Sia-specific binding compared to mock treatment (top panel; – periodate) (representative of two independent experiments). (c) NG stability after freeze–thaw was assessed by Sia surface expression analyzed by microarray. (d) NG stability was also measured by ELISA. Fresh and freeze–thawed NGs were printed with a NanoPrint arrayer at 40 μg protein/mL on an epoxide-coated glass slide (10 replicates per sample) or coated at 1 μg of protein/well to a 96-well plate in triplicate for ELISA. Samples were then analyzed as indicated with Bio-SNA, Bio-MAL-II, and anti-Neu5Gc IgY, detected by streptavidin and donkey-anti-chicken IgY [HRP-conjugated (c) or Cy3-conjugated (d)], respectively, demonstrating right-side-out orientation and stability after one freeze–thaw cycle (representative of at least two independent experiments; mean ± SD).

generate biomimetic glyconanoparticles that express Neu5Gc-TACA in their natural context, we used porcine-derived RBC that naturally express Neu5Gc-glycoconjugates due to their active CMAH enzyme. However, porcine also expresses the carbohydrate αGal (Galα1-3Galβ1-4GlcNAc-R) that is an immunogenic xenoantigen in humans and against which all humans have circulating anti-Gal antibodies.[42] To eliminate the αGal antigen, we used a porcine strain that is deficient in the *GGTA1* gene encoding the α1,3-galactosyltransferase (α1,3GT).[43] Thus, we used RBCs from two porcine knockout strains that express Neu5Gc-glycoconjugates (Neu5Gc^{pos}; *Ggta1*$^{-/-}$ knocked-out strain;[43] Gal-KO) or control glycoconjugates that lack Neu5Gc but instead express the nonimmunogenic Neu5Ac (Neu5Gc^{neg}; double-knocked-out *Ggta1*$^{-/-}$/*Cmah*$^{-/-}$ strain;[44] Gal/Gc-DKO) (Figure 1a). RBCs were first purified from fresh blood of these porcine knockout strains by centrifugation and PBS wash. Then isolated RBCs went through membrane rupture in a hypotonic buffer to remove the intracellular contents. Next, the emptied RBCs were washed and then resuspended to form glycoproteolipid nanoghost vesicles (NGs). These glyconanoparticles were designed to be biomimetic nanosized particles containing a glycan shell that mediates its immunogenic properties.

We next examined the physiochemical properties of these NGs biomimetic glyconanoparticles using Cryo transmission electron microscopy (cryo-TEM), showing a similar and uniform morphology of NGs that either express Neu5Gc (Neu5Gc^{pos}-NG; NG^{pos}) or lack its expression (Neu5Gc^{neg}-NG; NG^{neg}) (Figure 1b). Dynamic light scattering (DLS) indicated that both NG^{pos}/NG^{neg} had a similar zeta potential of approximately −25 mV (Figure 1c) and an average hydrodynamic diameter of ∼400 nm (Figure 1d,e).

Further biochemical characterization demonstrated similar protein content by silver staining (Figure 2a), containing all expected major RBC membrane protein bands.[40] Subsequently, the sialic acid (Sia) content was compared between the two NGs preparations by Western blot developed with the Sia-binding proteins: lectins that bind both Neu5Ac- and Neu5Gc- that are Siaα2–6-linked to underlying glycans (*Sambucus nigra Agglutinin*; SNA) or Siaα2–3-linked to

DOI: 10.1021/acsnano.8b07241
ACS Nano 2019, 13, 2936–2947

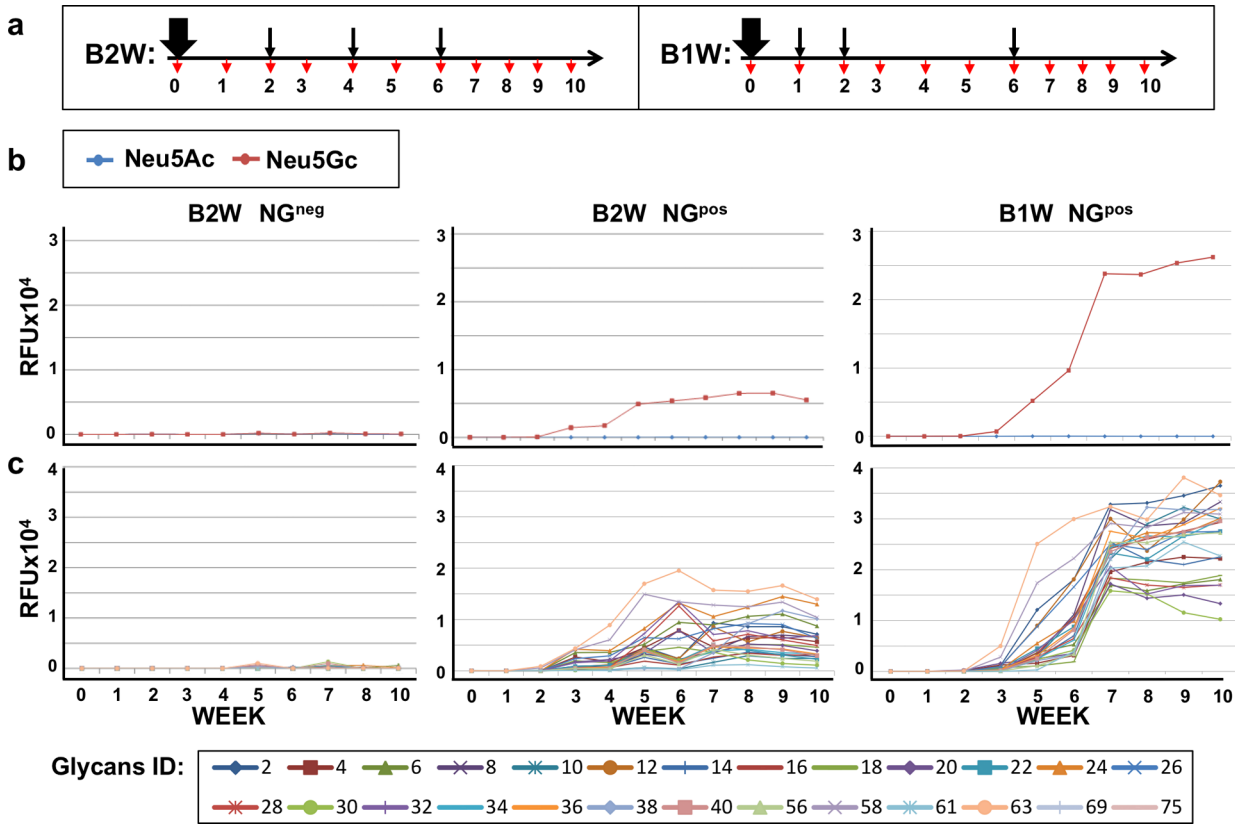

Figure 3. Optimization of vaccination regimen. (a) Schematic representation of the immunization regimen. *Cmah*$^{-/-}$ mice were immunized intraperitoneally (i.p.) with 200 μL of 1 μg/μL NG^{neg} or NG^{pos} (n = 7 per group) emulsified in Freud's Complete Adjuvant (FCA; thick black arrow) then boosted three times with NGs in Freud's Incomplete Adjuvant (FIA; thin black arrows) at initial 1 or 2 week intervals, as indicated (B1W, B2W, respectively). Mouse serum was sampled on day 0 then weekly (red arrows). Sera samples were then analyzed by sialoglycan microarrays containing diverse sialoglycans, detected with Cy3-labeled antimouse IgG. (b) Average IgG response of the 7 mice in each group is presented as average response against monosialylated Neu5Gc-glycans (n = 24; red) and Neu5Ac-glycans (n = 24; blue). (c) Array response against the 24 individual Neu5Gc-glycans (colored lines; full list of glycans in Supplementary Table 1).

underlying glycans (*Maackia Amurensis Lectin II*; MAL-II), and the polyclonal chicken-anti-Neu5Gc IgY that bind various Neu5Gc-containing glycans (Figure 2b).[45,46] Sia-specific binding was confirmed by mild periodate oxidation treatment that truncates two carbons off the Sia side chain, hence resulting in loss of Sia-binding.[47] This biochemical analysis revealed that parallel glycoprotein bands were stained with both SNA and MAL-II lectins, demonstrating both terminal Siaα2−6 and Siaα2−3, and supporting similar Sia content in both NG^{pos}/NG^{neg} (Figure 2b). Importantly, the Sia staining was mostly removed with periodate oxidation confirming Sia-specific recognition (Figure 2b). In addition, Neu5Gc was only present in NG^{pos} but not in NG^{neg}, and its staining was eliminated after treatment with periodate (Figure 2b). Taken together, these results indicate that the only difference between NG^{pos}/NG^{neg} preparations is the presence or lack of Neu5Gc expression, respectively. In fact, NG^{pos} contain diverse Neu5Gc-glycans, while NG^{neg} contain diverse Neu5Ac-glycans. Of note, the glycans on these two NGs preparations differ only by the additional hydroxyl group in glycans covered with Neu5Gc instead of Neu5Ac.

Surface Sia expression on NGs is critical for its application as a successful and reproducible active cancer vaccine. Once prepared, the NGs were kept frozen at −80 °C until further use. To monitor the stability of NGs after several freeze−thaw cycles, NGs were printed onto epoxide-activated glass slides using a nanoprinter, and then slides were developed with Sia-binding proteins. The results indicated that Sia content had not changed after one freeze−thaw cycle; however, SNA and anti-Neu5Gc IgY reactivity had been greatly reduced at the second and third freeze−thaw cycles, respectively (Figure 2c). This is likely due to NG degradation or inside-out flipping, both resulting in reduced expression of sialylated antigens. Similar results were obtained when freshly prepared, or once-thawed, NGs were coated onto an ELISA plate and examined with SNA, MAL-II, and anti-Neu5Gc IgY, demonstrating stable reactivity after one freeze−thaw cycle (Figure 2d). Therefore, to preserve their efficacy all NGs preparations had been aliquoted and used fresh or after only one freeze−thaw cycle in all subsequent studies.

NG Vaccination Allows Sustained and Robust Anti-Neu5Gc Antibody Response. Active vaccination can induce a sustained and broad immune response, given optimization of various factors, such as antigen immunogenicity, adjuvant, number of exposures and intervals between exposures.[48,49] To optimize the immunization protocol for sustained anti-Neu5Gc antibody response in mice, we first immunized *Cmah*$^{-/-}$ mice with NG^{pos} (Neu5Gc-glycans) or control NG^{neg} (Neu5Ac-glycans) emulsified in Freund's Complete Adjuvant (FCA), followed by two boost injections emulsified in Freund's Incomplete Adjuvant (FIA), at two-week intervals (B2W; Figure S1a).

Mouse sera were collected weekly, and then sera antibody response was evaluated by sialoglycan microarrays printed with

DOI: 10.1021/acsnano.8b07241
ACS Nano 2019, 13, 2936−2947

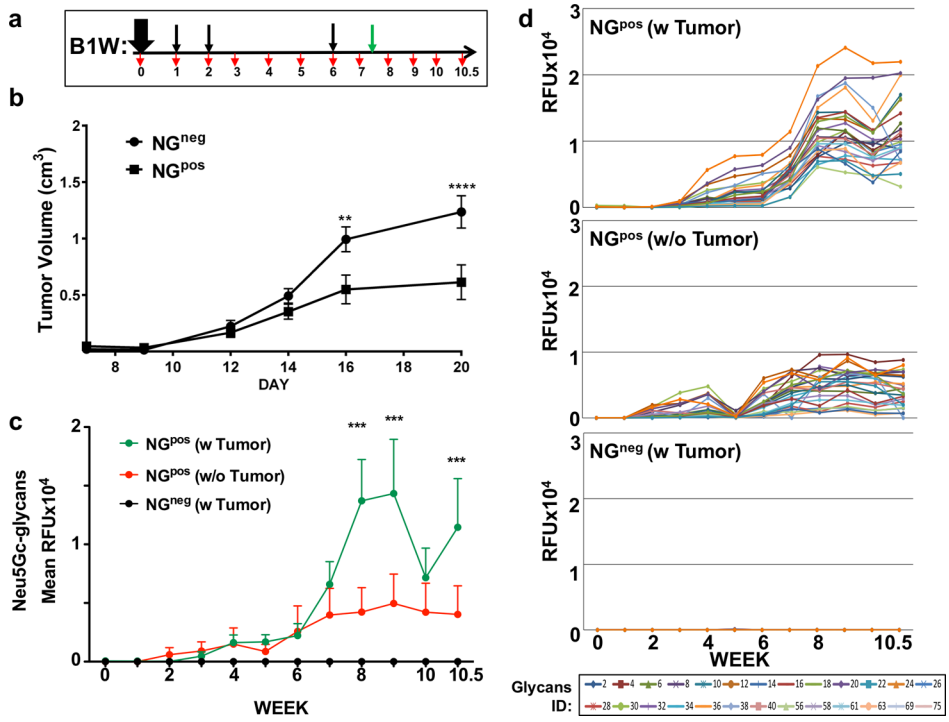

Figure 4. Cancer vaccine inhibit tumor growth *in vivo*. (a) Schematic representation of experimental design. *Cmah*$^{-/-}$ mice were immunized intraperitoneally (i.p.) with NG^{neg} or NG^{pos} (n = 10 per group) in the optimized B1W regimen. Mouse serum was sampled on day 0 then weekly (red arrows). On week 7.5, 0.5 × 10^6 MC38-GFP cells were inoculated subcutaneously (green arrow). (b) Tumor volumes were monitored every other day showing inhibition of tumor growth in the NG^{pos} vaccine-treated group (mean ± SEM; One-Way ANOVA with Bonferroni posttests, ** $p < 0.01$, *** $p < 0.001$; in NG^{pos} group, two mice became necrotic on week 10 and were excluded from analysis). (c) Sera samples were then analyzed by sialoglycan microarrays containing diverse sialoglycans, detected with Cy3-labeled antimouse IgG. Each line represents the average response of 10 mice per group against all Neu5Gc-glycans. (d) Array response agaisns the 24 individual Neu5Gc-glycans (colored lines).

a diverse collection of Neu5Gc-glycans and Neu5Ac-glycans. This analysis showed an IgG response against only some of the Neu5Gc-glycans, which had dropped to baseline at week 6, 2 weeks after the second boost (Figure S1b,c). Adding a third boost at week 6 slightly improved the diversity of anti-Neu5Gc IgG response, which was also sustained through week 10 (B2W; Figure 3). In both immunization protocols (B2W, 2 or 3 boosts), there was a complete absence of response against any of the Neu5Ac-glycans, which differ by only a single oxygen atom from their counterpart Neu5Gc-glycans (Figure S1 and Figure 3). Similarly, immunization with the control NG^{neg} (Neu5Ac-glycans) did not show any response against both Neu5Ac/Neu5Gc-glycans (Figure 3). These results exemplify the tolerance against the native Neu5Ac-glycans, in contrast to the high immunogenicity of Neu5Gc-glycans.

Adjuvants can enhance and shape vaccine immune responses, and vaccine schedules can dramatically affect antibody magnitude and persistence, with longer intervals between injections generally yielding greater responses.[48] To evaluate the contribution of the adjuvant to the developed response in mice, *Cmah*$^{-/-}$ mice were immunized (B2W, two boosts) with NG^{pos} or NG^{neg}, with or without adjuvant. Analysis of sera obtained at week 6 revealed a clear contribution of the adjuvant to the level and diversity of the developed anti-Neu5Gc IgG response (Figure S2). Next, the interval between boost injections was further optimized and persistence of response evaluated. *Cmah*$^{-/-}$ mice were immunized with NG^{pos} in FCA, then with two boost injections in FIA after 1 and 2 weeks, followed by a third boost 6 weeks after primary immunization (B1W; Figure 3a). Glycan microarray analysis revealed a highly diverse, robust, and persistent anti-Neu5Gc IgG response that remained high even 10 weeks post primary immunization (Figure 3b). Boosting with the Neu5Gc-deficient NG^{neg}-FIA after primary immunization (Figure S3a) showed a much lower anti-Neu5Gc response compared to boosting with NG^{pos}-FIA (Figure S3b), while this change had no effect on the developed immune response against the NG-carrier that was similar between the two boosting regimens (Figure S3c). Hence, the presence of Neu5Gc during boosting is important for the development of anti-Neu5Gc response. Overall, the B1W vaccination regimen (weeks 0, 1, 2, 6) with NG^{pos} boosting had proved to be more efficient than B2W (weeks 0, 2, 4, 6), yielding a high and specific anti-Neu5Gc IgG response that was sustained for at least 4 weeks after the third boost.

Evaluating Cancer Vaccine Efficacy against Neu5Gc-Positive Tumors. Previous studies showed that treatment of Neu5Gc-positive tumors with passively transferred human[34] or mouse[35] anti-Neu5Gc antibodies in the Neu5Gc-deficient *Cmah*$^{-/-}$ mouse model have dualistic and contrasting responses.[34,50,51] While high doses of anti-Neu5Gc antibodies inhibited tumor growth,[34] a low dose treatment actually promoted tumor growth.[34,52,53] Furthermore, the shift between these opposite dosage effects occurred at a very narrow range, of even only 2-fold changes.[35] As such, anti-Neu5Gc antibodies are both cancer biomarkers and potential therapeutics.[34,54]

To evaluate the active vaccination at a low quality of response, mice were immunized with NG^{pos} or NG^{neg} at the

DOI: 10.1021/acsnano.8b07241
ACS Nano 2019, 13, 2936−2947

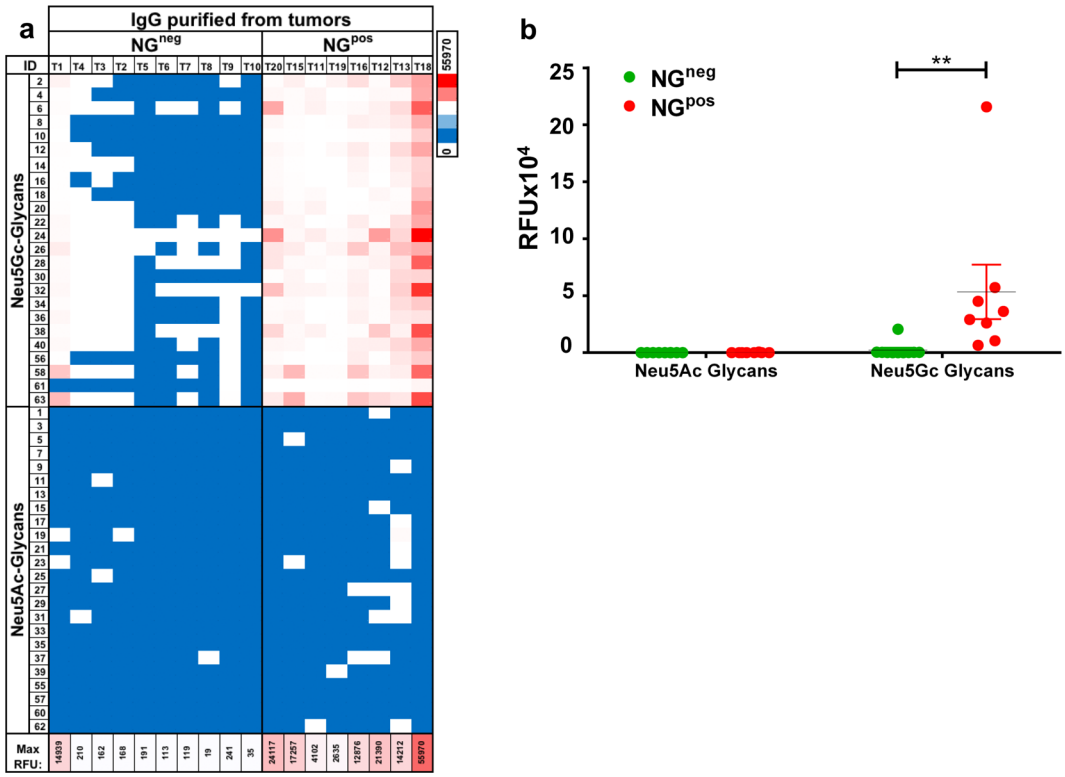

Figure 5. Intratumoral IgG recognize Neu5Gc-glycans. (a) Tumors were harvested from vaccine or control-immunized mice (NG^{pos} or NG^{neg}, respectively) and minced, and then IgG antibodies were purified with Protein-A. A 20 ng/μL sample of intratumoral purified IgG antibodies was analyzed on sialoglycan microarrays and then detected by Cy3-antimouse IgG. Results are presented as heat map of IgG reactivity in relative fluorescent units (RFU), per glycan per mouse, against the collection of Neu5Gc-glycans or Neu5Ac-glycans (blue−white−red scale represent 0−50−100 percentiles). (b) Average IgG response of individual mice against Neu5Gc-glycan or Neu5Ac-glycans on microarray (Two-Way ANOVA with Bonferroni post-tests, ** $p < 0.01$).

nonoptimal B2W regimen (weeks 0, 2, 4; Figure S4a), and then syngeneic Neu5Gc-positive tumors (mouse adenocarcinoma MC-38) were inoculated subcutaneously at week 5.5 and tumor growth monitored. While NG^{pos}-vaccinated mice showed a slight decrease in tumor growth compared to NG^{neg}-vaccinated group, this trend was not statistically significant (Figure S4b). Nevertheless, it was encouraging to find that, unlike passive therapy,[34,35] even at a low quality of anti-Neu5Gc antibodies response (Figure S1), active vaccination did not mediate promotion of tumor growth, suggesting that the active vaccine is safe with respect to the negative low dose effects.

Next, we evaluated the therapeutic efficacy of the optimized active vaccine regimen and its effect on tumor growth *in vivo*. Mice were immunized with NG^{pos} or NG^{neg} at the optimal B1W regimen (weeks 0, 1, 2, 6), syngeneic Neu5Gc-positive MC-38 tumor cells were inoculated subcutaneously at week 7.5, and then tumor growth and antibodies responses monitored (Figure 4a). In this case, tumor growth was dramatically inhibited in the vaccine-treated group (NG^{pos}) compared to the control-treated group (NG^{neg}) (Figure 4b). All groups showed minimal serum IgM/IgG responses against the NG^{neg}-carrier but higher response against NG^{pos}-carrier that is likely mediated by its immunogenic Neu5Gc component (Figure S5). Detailed glycan microarray analysis revealed that following NG^{pos} vaccination, exposure to the inoculated Neu5Gc-positive tumors at week 7.5 mediated a dramatic enhancement in the average anti-Neu5Gc IgG response, compared to the group that had not been exposed to the tumors (Figure 4c). This reflected an increase in antibody binding reactivity against all examined Neu5Gc-glycans (Figure 4d), likely also representing an increase in the affinities of these antibodies.[55] In contrast, the inoculated tumors had no effect on the developed anti-Neu5Gc IgMs response (Figure S6) that had dramatically increased immediately after the third boost on week 6, even before tumor inoculation, then remained static for 2 weeks (Figure S6b). Importantly, the control NG^{neg} treatment did not result in any serum response against Neu5Gc-glycans, even after tumor inoculation (Figure 4c,d).

In humans when tumors develop later in life, the continued consumption of dietary Neu5Gc (red meat, dairy) results in its preferential accumulation on developed tumor cells[32] due to their higher metabolism and elevated expression of Sialin, a sialic acid transporter.[56] Therefore, anti-Neu5Gc antibodies boosted response by Neu5Gc-positive tumors is likely to occur also in humans. In fact, it had been shown that some anti-Neu5Gc antibodies are elevated in carcinoma patients and can be used as cancer biomarkers.[34,54]

Characterization of Purified Intratumoral IgG. Anti-Neu5Gc antibodies developed during the cancer vaccine treatment clearly play an important role in its therapeutic efficacy (Figure 4). One of the ways antibodies mediate tumor growth inhibition and/or killing is by directly binding to their target antigens expressed on the surface of tumor cells.[57,58] While NG^{pos} vaccine-treated mice showed tumor anti-Neu5Gc IgG boosting effect on weeks 8 and 9, noticeably, they also displayed a transient depletion of serum anti-Neu5Gc IgG on

DOI: 10.1021/acsnano.8b07241
ACS Nano 2019, 13, 2936−2947

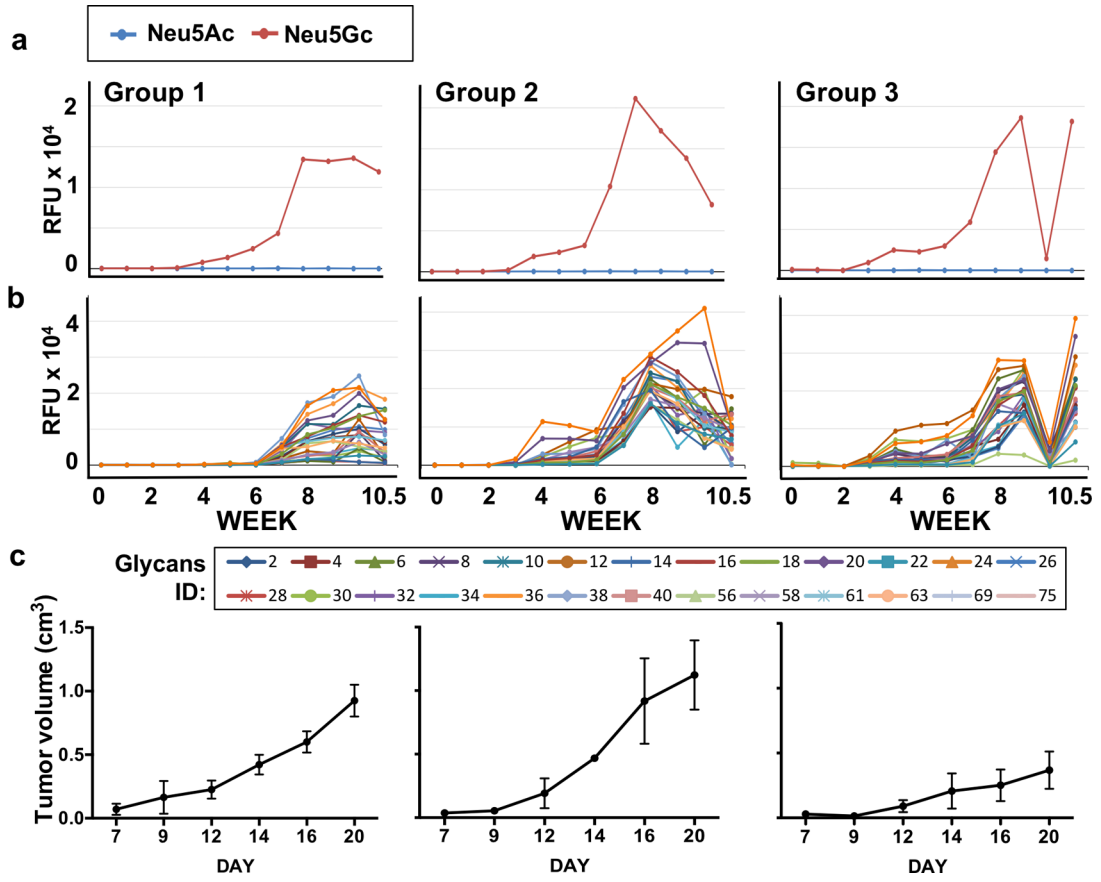

Figure 6. Kinetics of anti-Neu5Gc IgG response and tumor growth in vaccine treated mice. Glycan microarray analysis and tumor growth kinetics in mice of the vaccine treated group that was inoculated with tumors (NG^{pos} w/Tumor; B1W; Figure 4). These mice were divided into three group types, according to their antibodies and tumor volume kinetic of response. (a) Average IgG response against all Neu5Gc-glycans and all Neu5Ac-glycans, per group. (b) Average IgG response against individual Neu5Gc-glycans, per group. (c) Average of tumor growth kinetics, per group.

week 10 (2.5 weeks after tumor inoculation) that was not observed in the vaccine-treated group without inoculation of tumors (Figure 4c). The drop in average response reflected a similar trend in the response to almost all individual Neu5Gc-glycans (Figure 4d). To evaluate the hypothesis that these antibodies had migrated to the tumors, tumors were harvested and minced into suspension, and then intratumoral antibodies were purified by protein A to capture IgG antibodies. Glycan microarray analysis of purified intratumoral IgGs revealed that all vaccine-treated mice (NG^{pos}) had a strong and highly specific binding reactivity against all Neu5Gc-glycans but not Neu5Ac-glycans (Figure 5a,b), supporting migration of serum anti-Neu5Gc IgGs into the growing tumor mass. On the other hand, antibodies purified from tumors of control vaccination (NG^{neg}; n = 10) showed mostly very low reactivity on the arrays (Figure 5a,b). Interestingly, few mice in this control group had a very low but specific anti-Neu5Gc IgG response, likely mediated by the tumors that present foreign Neu5Gc-neoantigens. Notably, although MC-38 tumor cells express more Siaα2−3-linked than Siaα2−6-linked sialic acids,[35] no notable difference was detected in the epitopes recognized by the purified intratumoral IgG. Both vaccine and control treated mice showed similar infiltration of immune cells ($CD45^+$ and $CD45^+CD3^+$; Figure S7). Altogether, these results suggest that anti-Neu5Gc IgG antibodies reach the tumor mass to mediate inhibition of tumor growth.

Evaluating Heterogeneity in Vaccine Treatment. A key feature of vaccine therapy is the heterogeneity in the developed immune responses of different individuals to a given vaccine in both the magnitude and decay rate of responses, as well as of a given individual to different vaccines.[59,60] In cancer vaccine technology, tumor heterogeneity adds another level of complexity.[61] To evaluate heterogeneity in NG^{pos} vaccination treatment, the kinetics of anti-Neu5Gc IgG responses and tumor growth were monitored in each mouse individually (Figure S8). This analysis revealed three types of responses (Figure S8 and Figure 6). Group 1 showed a late onset of response around weeks 6−7, with intermediate magnitude of response and a low therapeutic effect on tumor. Group 2 showed a two-phase response initiating around weeks 3−4, followed by a secondary response immediately after the third boost vaccination on week 6 that had gradually decayed, with no therapeutic effect on tumors. By contrast, group 3 showed a dramatic tumor inhibiting therapeutic effect with a distinct pattern of antibody kinetics. In this group, there was a two-phase response as in group 2; however in addition, there was an almost complete depletion of anti-Neu5Gc IgG from the serum on week 10 that was restored a few days later by week 10.5 (Figure S8 and Figure 6). Furthermore, only in group 3 did the IgG titer seem to be higher than the IgM (Figure S8d). This analysis clearly demonstrated that certain immune response kinetics, as developed in group 3, are more

DOI: 10.1021/acsnano.8b07241
ACS Nano 2019, 13, 2936−2947

constructive in supporting the therapeutic effects mediated by the cancer vaccine.

CONCLUSIONS

While envisioned already in 1891,[62] only a few cancer vaccines have been approved by the US Food and Drug Administration (FDA) thus far.[13,61] The key barriers to their success are low antigenicity of targeting antigens, tumor heterogeneity,[61] and low mutational burden with only few peptide neoantigens in some cancers.[63] These limitations prompted the continued search for other potential antigens for vaccines.[64] Tumor-associated glycosylation changes generate carbohydrate−neoantigens that are excellent candidate targets for immunotherapy.[28,65] In particular, Neu5Gc, the antigenic non-human dietary carbohydrate that accumulates on human carcinoma,[66,67] generates a whole array of cancer neoantigens.[34,35]

Red blood cells have been investigated for over 40 years as potential antigen delivery systems,[68−70] with some success in human patients,[71] and more recently as drug delivery vehicles,[72] including in nanostructured biomedical systems.[36−38] Here, we designed an active cancer vaccine targeting Neu5Gc-TACAs in a mouse model, as a proof of concept. Taking advantage of RBC biocompatibility and expected prolonged circulation time,[37,39,73] glyconanoparticles were prepared from engineered porcine erythrocytes membranes. These biomimetics were used to actively vaccinate "human-like" Neu5Gc-deficient mice after optimization of adjuvant and immunization schedules. The engineered NGs were designed to operate as a cancer vaccine to mount an effective immune response against cancer and therefore were not expected to reach the tumor mass in order to facilitate killing. Taking advantage of the glycan microarray technology for biomedical antibody profiling,[45,65,74−76] full analysis of responses against 48 different sialoglycans revealed a highly specific, robust, and prolonged anti-Neu5Gc IgGs with distinctive patterns of humoral responses in individual mice. Neu5Gc-positive tumors further enhanced the vaccine-developed humoral anti-Neu5Gc responses, as also expected in humans,[34] and the vaccine treatment inhibited tumor growth. Interestingly, 37.5% of mice optimally responded to the vaccine therapy and revealed a specific pattern of antibody response kinetics that included their complete, but transient, depletion from circulation. This important kinetic feature can contribute to understanding the heterogeneity of responses to vaccines and assist in prediction of responses.[77] While the current investigation was focused on the antibodies responses, it is likely that the cellular arm of the immune system also participates in the successful therapeutic effects,[78−80] which would warrant cellular immune profiling in the future.

METHODS

Materials. Dulbecco's Modified Eagle's Medium high glucose (DMEM), fetal bovine serum (FCS), L-glutamine, and penicillin−streptomycin (pen−strep) Dulbecco's PBS were all purchased from biological industries; Trizma-hydrochloride, Tween-20, Ovalbumin (Grade V), *O*-phenylenediamine (OPD), and periodate were all purchased from Sigma-Aldrich; EDTA was purchased from Fisher Scientifics; hydrogen peroxide 30% was purchased from Merck.

Antibodies and Lectins. Chicken anti-Neu5Gc IgY (Biolegend), biotinylated-SNA, biotinylated-MALII (Vector Lab), HRP-donkey-anti-chicken IgY, HRP-streptavidin, Cy3-goat-anti-mouse IgG, Cy3-donkey-anti-chicken IgY, and Cy3-Strepavidin (Jackson ImmunoResearch) were all from commercial sources.

Cell Lines and Mice. MC38-GFP cells (murine colon adenocarcinoma cells stably expressing GFP,[81] kindly provided by Prof. Ajit Varki) were grown in culture (DMEM with high glucose, 10% FCS, 1% glutamine, 1% penn−strep). *Cmah*$^{-/-}$ mice were bred and maintained according to the Animal Care and Use Committee protocol approved by Tel Aviv University.

Generation of Nanoghost Glyconanoparticles from Porcine Red Blood Cells. NGs were prepared from porcine red blood cells (RBC) of two strains: α-Gal *Ggta1*$^{-/-}$ knocked-out[43] and the double-KO *Ggta1*$^{-/-}$/*Cmah*$^{-/-}$[44] (Gal/Gc-DKO; Neu5Gc-Negative; NG^{neg}) strains. RBC were packed by three rounds of centrifugation in PBS pH 7.4 (1000*g*, 10 min) and then stored at −80 °C until further use. Packed RBCs (2.5 mL) were lysed by incubation on ice with 25 mL of ice-cold lysis buffer (50 mM of Tris−HCl, pH 7.35 containing 10 mM of EDTA) for 10 min and then centrifuged for 30 min at 26000*g* with no brakes (to avoid pellet detachment). The supernatant was removed, and the lysis procedure was repeated until the NG pellet became white. The NG pellet was washed with 25 mL of ice-cold doubledistilled H_2O (DDW) and then resuspended in 1 mL DDW. Protein content was determined by BCA (Pierce), the volume was adjusted to a final concentration of 2 mg/mL, and then 1 mL aliquots were stored at −80 °C until further use. For physical characterization, NGs were stored at 4 °C and analyzed within 24 h of preparation.

Cryo Transmission Electron Microscopy (cryo-TEM). NGs were diluted to 0.1 mg/mL, and aliquots of 5 μL each were pipetted onto a plasma-etched (25 s) 200 mesh holey carbon grid (PELCO) held in the plunge chamber at approximate 90% humidity. Sample preparation was carried out using a Cryo-Plunge 3 unit (Gatan Instruments) employing a double blot technique. The samples were blotted for 2 s and then plunged into liquid ethane at a temperature of −170 °C. After vitrification, the grids were transferred under liquid nitrogen to the cryo-TEM specimen holder (Gatan 626 cryo holder) at −170 °C. Imaging was carried out using a Tecnai G2 cryo-TEM (FEI Co., Eindhoven, Netherlands) operated at 120 kV with a Gatan 4000 camera, and images were captured using Digital Micrograph software (Gatan). During imaging, the temperature of the sample holder was maintained at −170 °C to minimize sublimation of vitreous water.

Dynamic Light Scattering To Determine Size and Zeta Potential. Freshly prepared NGs were diluted in PBS pH 7.4 (for size) or water (for zeta potential) to 20 μg/mL total protein and measured in a Malvern Nano ZS zetasizer. Data calculations were performed using the Zetasizer software with the Intensity algorithm. Each experimental result is an average of at least three independent measurements. Error bars represented mean ± SD, with size SD calculated by multiplying the mean size with the square root of the PDI (polydispersity index).

Protein Analysis of NGs by Silver Staining. Freshly prepared NGs were diluted in SDS sample buffer to 40 ng/μL, incubated at room temperature (rt) for 30 min, and then separated on 12% SDS−PAGE gels. Gels were fixed for 20 min at rt in 25 mL of fixation solution 1 (10% acetic acid, 40% ethanol, 50% DDW, 0.0185% formaldehyde), washed three times with 50% ethanol for 10 min each, sensitized for 1 min with 25 mL of 0.02% $Na_2S_2O_3$ in DDW, washed with water for 20 s 3 times, incubated for 12 min with 25 mL of silver nitrate solution (9.4 mM AgNO containing 0.02% formaldehyde), and washed three times with water for 20 s each. Gels were developed using a developing solution (0.0005% $Na_2S_2O_3$, 0.015% formaldehyde, 5% Na_2CO_3) until bands appeared and then stopped with fixation solution 2 (10% acetic acid, 40% ethanol, 50% DDW), and gels were scanned.

Sialic Acid Content Analysis of NGs by Western Blotting. Sialic acid content was evaluated by lectin analysis of Western blots. Freshly prepared NGs were diluted in SDS sample buffer to 40 ng/μL, incubated at room temperature for 30 min, and then separated on 12% SDS−PAGE gels followed by transfer onto a nitrocellulose membrane (Whatman, GE Life Technologies). Membranes were blocked with TBST (50 mM Tris pH 7.6, 0.15 M NaCl, 0.1 Tween-20) supplemented with 2% fish gelatin (Sigma) for 1 h at rt with gentle shaking, washed three times with TBST, and incubated with

DOI: 10.1021/acsnano.8b07241
ACS Nano 2019, 13, 2936−2947

primary detection for 1 h at rt (either 1/7000 diluted chicken anti-Neu5Gc IgY or biotinylated lectins; Bio-SNA diluted to 0.4 μg/mL and Bio-MALII diluted to 4 μg/mL, as described in the figure legends). Next, membranes were washed three times with TBST and incubated with secondary detection (HRP-donkey-anti-chicken IgY 0.16 μg/mL or HRP-Streptavidin 0.1 μg/mL, respectively) for 1 h at rt. Membranes were developed using an enhanced chemiluminescence kit (ECL; Pierce).

Sialic Acid Specificity Analysis by Mild Periodate Oxidation Treatment. Freshly prepared NGs were diluted in SDS sample buffer to 40 ng/μL and incubated at room temperature for 30 min. The samples were separated on 12% SDS−PAGE gels, followed by transfer onto nitrocellulose membrane (Whatman, GE Life Technologies). Membranes were washed three times with ice-cold water, once with ice-cold PBS pH 6.5 (8.7 mM NaH_2PO_4, 137 mM NaCl), and then incubated for 30 min with 2 mM of periodate diluted in PBS 6.5 at rt while protected from light. Then the membranes were washed six times with water and further analyzed by Western blotting, as described above.

Sialic Acid Analysis by Lectin ELISA. NGs were coated onto 96-well microtiter plates (Costar, Corning) in duplicates at 1 μg protein/well in 50 mM sodium carbonate−bicarbonate buffer, pH 9.5, and incubated overnight at 4 °C. Wells were blocked for 1 h at rt with blocking buffer (PBS pH 7.4 with 1% ovalbumin) and then aspirated and incubated with diluted primary antibody (chicken anti-Neu5Gc IgY at 1/1000, biotinylated SNA or MAL-II at 1 μg/mL) at 100 μL/well in the same blocking buffer for 2 h at rt. Plates were washed three times with PBST (PBS pH 7.4, 0.1% Tween-20) and then incubated for 1 h at rt with HRP-conjugated secondary antibody (HRP-donkey-anti-chicken IgY 0.26 μg/mL or HRP-streptavidin 0.1 μg/mL, respectively) in PBS. After being washed three times with PBST, wells were developed with 140 μL of *O*-phenylenediamine in 100 mM of citrate−PO_4 buffer, pH 5.5, and the reaction was stopped with 40 μL of H_2SO_4 (4 M). Absorbance was measured at 490 nm on SpectraMax M3 (Molecular Devices). Specific binding was defined by subtracting the background readings obtained with the secondary antibody only on coated wells.

Sialoglycan Microarray Fabrication. Arrays were printed as described.[45] Briefly, arrays were fabricated with NanoPrint LM-60 Microarray Printer (Arrayit, CA) on epoxide-derivatized slides (Corning) with 16 subarray blocks on each slide. Glycans were distributed into one 384-well source plates with four replicate wells per sample and 8 μL per well (Version 1.0). Each glycan was prepared at 100 μM in an optimized print buffer (300 mM phosphate buffer, pH 8.4). To monitor printing quality, replicate wells of mouse IgG (Jackson ImmunoResearch, at 200, 100, 50, 25, 12.5, 6.25 ng/μL in PBS+10% glycerol) and AlexaFlour-555-Hydraside (Invitrogen, at 1 ng/μL in 178 mM phosphate buffer, pH 5.5) were used for each printing run. The arrays were printed with four 946MP3 pins (5 μm tip, 0.25 μL sample channel, ∼100 μm spot diameter; Arrayit, CA). Each block (subarray) had 17 spots/row, 20 columns with spot-to-spot spacing of 225 μm. The humidity level in the arraying chamber was maintained at about 66% during printing. Printed slides were left on arrayer deck overnight, allowing the humidity to drop to ambient levels (40−45%). Next, slides were packed, vacuum-sealed, and stored at rt in a desiccant chamber until further use. Slides were printed in one batch of 56 slides.

NGs Stability Analysis Using Microarray. Arrays were printed using a NanoPrint LM-60 microarray printer (Arrayit, CA) on epoxide-derivatized slides (Corning) with 16 subarray blocks on each slide. Glycans and freshly prepared NGs diluted to 40 ng/μL in 187 mM phosphate buffer pH 8.4 were distributed into one 384-well source plate with four replicate wells per sample and 8 μL per well. In addition, in order to investigate the stability of NGs, samples (40 μL from each NG preparation) were frozen for 5 min in −80 °C, quickly thawed, and diluted to 40 ng/μL. This cycle was repeated twice, and the diluted samples were printed as well. Synthetic glycans were also printed and diluted to 100 μM in 300 mM phosphate buffer, pH 8.4. To monitor printing quality, AlexaFlour-555-Hydraside (Invitrogen, at 1 ng/μL in 178 mM phosphate buffer, pH 5.5) was used for each printing run. The arrays were printed using 4 SMP3 pin (5 μm tip, 0.25 μL sample channel, ∼100 μm spot diameter; Arrayit, CA). Each block (subarray) had 16 rows and 10 columns with spot-to-spot spacing of 225 μm. The humidity level in the arraying chamber was maintained at about 70% during printing. Printed slides were left on the arrayer deck overnight, allowing the humidity to drop to ambient levels (40−45%). Next, slides were packed, vacuum-sealed, and stored at rt in a desiccant chamber until further use. Slides were developed using antibodies and lectins as described below and in the relevant figure legend.

Evaluating Anti-NG Response in Immunized Mice Using Microarray. Arrays were printed using NanoPrint LM-60 microarray printer (Arrayit, CA) on epoxide-derivatized slides (Corning) with 16 subarray blocks on each slide. NGs as well as synthetic glycans were distributed into one 384-well source plate with four replicate wells per sample and 8 μL per well. Each NG sample was diluted in PBS pH 7.4 to 100 ng/μL and synthetic glycans at 100 μM in 300 mM phosphate buffer, pH 8.4. To monitor printing quality, mouse IgG (Jackson ImmunoResearch) at 40 ng/μL in PBS + 10% glycerol and AlexaFlour-555-Hydraside (Invitrogen, at 1 ng/μL in 178 mM phosphate buffer, pH 5.5) were used for each printing run. The arrays were printed using one SMP3 pin (5 μm tip, 0.25 μL sample channel, ∼100 μm spot diameter; Arrayit, CA). Each block (subarray) had 14 rows and 6 columns with spot-to-spot spacing of 225 μm. The humidity level in the arraying chamber was maintained at about 70% during printing. Printed slides were left on the arrayer deck overnight, allowing the humidity to drop to ambient levels (40−45%). Next, slides were packed, vacuum-sealed, and stored at rt in a desiccant chamber until further use. Slides were developed using antibodies and lectins as described below and in the relevant figure legend.

Glycan Microarray Binding Assay. Slides were developed and analyzed as previously described.[45] Slides were rehydrated with dH_2O and incubated for 30 min in a staining dish with 50 °C prewarmed 0.05 M ethanolamine in 0.1 M of Tris−HCl, pH 9.0, to block the remaining reactive epoxy groups on the slide surface and then washed with 50 °C prewarmed dH_2O. Slides were centrifuged at 200*g* for 3 min and then fitted with a ProPlate Multi-Array 16-well slide module (Invitrogen) to divide into the 16 subarrays (blocks). Slides were washed with PBST (PBS pH 7.4, 0.1% Tween-20), aspirated, and blocked with 200 μL/subarray of blocking buffer (PBS/OVA; PBS pH 7.4, 1% ovalbumin) for 1 h at rt with gentle shaking. Next, the blocking solution was aspirated, 100 μL/block of primary detection (1/100 mice sera, or 1/7000 chicken anti-Neu5Gc IgY, or Bio-SNA 20 ng/μL) diluted in PBS/OVA was added, and then slides were incubated at rt with gentle shaking for 2 h. Slides were washed three times with PBST and then with PBS for 5 min/wash with shaking. Bound antibodies were detected by incubation with secondary detection (Cy3-goat-antimouse IgG 1.5 μg/mL, or Cy3-donkey-antichicken IgY 1.5 μg/mL, or Cy3-Streptavidin 1.2 μg/mL) diluted in PBS added at 200 μL/block and then incubated at rt for 1 h. Slides were washed three times with PBST and then with PBS for 5 min/wash followed by removal from a ProPlate multi-array slide module and then immediately dipped in a staining dish with dH_2O and incubated for 10 min with shaking followed by centrifugation at 200*g* for 5 min. Dry slides were vacuum-sealed and stored in the dark until scanning.

Array Slide Processing. Processed slides were scanned and analyzed as described at 10 μm resolution with a Genepix 4000B microarray scanner (Molecular Devices) using 350 gain.[45] Images were analyzed by Genepix Pro 6.0 software (Molecular Devices). Spots were defined as circular features with a variable radius, and local background subtraction was performed. Data were analyzed by Excel.

Optimizing Cancer Vaccine Mouse Immunization Protocol. All animal experiments were conducted according to the guidelines of the Tel-Aviv University Institutional Animal Care and Use Committee. *Cmah*$^{-/-}$ mice 6−10 weeks old were i.p. immunized with either NG^{pos} or NG^{neg}. NGs at 2 mg/mL protein concentration were mixed 1:1 (by volume) with Freund's complete adjuvant (FCA) or Freund's incomplete adjuvant (FIA) until emulsified, and then 200 μL was injected intraperitoneally (i.p.; 200 μg NG/mouse). In the

DOI: 10.1021/acsnano.8b07241
ACS Nano 2019, 13, 2936−2947

first immunization protocol (B2W; n = 10), FCA i.p. immunization at week 0 was followed by two or three boost immunizations with FIA at two-week intervals (weeks 2, 4, 6; Figure 3A). In the second immunization protocol (B1W; n = 10), FCA i.p. immunization at week 0 was followed by two boost immunizations with FIA at one-week intervals (weeks 1, 2), followed by another boost at week 6 (Figure 3A). To evaluate the developed anti-Neu5Gc antibodies response and kinetics, mice were bled (facial vein) on a weekly basis, collecting tubes were incubated overnight at 4 °C and then centrifuged at 17000g for 2 min, and the serum was collected. Samples were stored at −80 °C until analysis by glycan microarray assays.

To evaluate the significance of Freund's adjuvant for the development of IgG antibodies, mice were immunized according to B2W protocol with 200 μg of either NG^{pos} or NG^{neg} in FCA/FIA (n = 7 per group) or NG^{pos} in PBS only (n = 7). Serum was collected as described above before the first injection and 2 weeks after the second boost (at week 6).

Evaluating Cancer Vaccine Efficacy *in Vivo*. MC38-GFP cells (murine colon adenocarcinoma cells stably expressing GFP)[81] were grown in culture (DMEM with high glucose, 10% FCS, 1% glutamine, 1% penn-strep) to 80% confluence, lifted with PBS/EDTA (10 mM EDTA in PBS without Ca^{2+}/Mg^{2+}) and then centrifuged at 1500g for 5 min at 4 °C and resuspended in DPBS. On week 7.5 after cancer vaccine (NG^{pos}) or control immunization (NG^{neg}), with either B2W or B1W protocols, $Cmah^{-/-}$ mice were subcutaneously injected at the flank with 0.5 × 10^6 MC38-GFP cells/mouse in 150 μL of DPBS. Tumors were palpable 5 days later and were measured every other day using a digital caliper, and then tumor volumes calculated [(height × length × width)/2].

To evaluate the effect of low levels anti-Neu5Gc antibodies on tumor progression, $Cmah^{-/-}$ mice were immunized with 200 μg of either cancer vaccine (NG^{pos}) or control immunization (NG^{neg}) using the B2W protocol with only two FIA boost immunizations (weeks 2 and 4), and 1 week later (week 5), mice were inoculated with 0.5 × 10^6 MC38-GFP cells/mouse and then monitored as described above.

Preparation of Intratumoral IgG. Tumors from cancer vaccine or control treated mice were harvested on day 21, sliced to small pieces (~2 mm), and incubated in DMEM with collagenase type II (1 mg/mL) and DNase-I (0.5 mg/mL) at 37 °C for 30 min (total volume of 3.5 mL/sample). The suspension was centrifuged for 10 min at 400g, and the supernatants were collected and then again centrifuged at 400g for 5 min. The resulting supernatants were transferred to 15 mL tubes, and 50 μL of prewashed protein A Sepharose 4 Fast Flow beads (GE Healthcare) were added to each tube. Samples were incubated at 4 °C for 48 h while mixing and then loaded on a polyprep column (BioRad), washed three times with PBS, and eluted with 0.5 mL 0.1 M glycine, pH 2.5 into tubes containing 120 μL of Tris−HCl buffer (1 M, pH 9.0). Purified IgG antibodies were stored at 4 °C until analyzed by glycan microarray assays.

Statistical Analysis. One-way or two-way analysis of variance (ANOVA) tests for multiple comparison, or t tests, were performed using Graphpad Prism software (version 6). The results are expressed as mean ± STD or SEM (as indicated in the figure legends).

ASSOCIATED CONTENT

Supporting Information

The Supporting Information is available free of charge on the ACS Publications website at DOI: 10.1021/acsnano.8b07241.

Supporting figures (PDF)

Glycan array data (XLSX)

AUTHOR INFORMATION

Corresponding Author

*Tel: +972-3-640-6737. Fax: +972-3-642-2046. E-mail: vkaravani@tauex.tau.ac.il.

ORCID

Hai Yu: 0000-0002-4378-0532

Xi Chen: 0000-0002-3160-614X

Vered Padler-Karavani: 0000-0002-4761-3571

Author Contributions

V.P.-K. designed the experiments and supervised the project. E.M.R. and S.L.B.-A. performed the research; H.Y., R.D., A.P., S.C., J-P.S., C.G., and X.C. provided crucial reagents; S.B.A analyzed FACS of immune cells. E.M.R., S.L.B-A., and V.P.-K. wrote the paper, and all authors read and approved the manuscript.

Author Contributions

#E.M.R. and S.L.B.-A. contributed equally.

Notes

The authors declare no competing financial interest.

ACKNOWLEDGMENTS

This work was supported by a European Union H2020 Program grant (ERC-2016-STG-716220) (to V.P.-K.). Gal-KO pigs were kindly obtained from D. Sachs, TBRC, Boston.

REFERENCES

(1) Lesterhuis, W. J.; Haanen, J. B.; Punt, C. J. Cancer Immunotherapy–revisited. *Nat. Rev. Drug Discovery* **2011**, *10*, 591−600.

(2) Pardoll, D.; Allison, J. Cancer Immunotherapy: Breaking the Barriers to Harvest the Crop. *Nat. Med.* **2004**, *10*, 887−892.

(3) Chen, D. S.; Mellman, I. Oncology Meets Immunology: The Cancer-Immunity Cycle. *Immunity* **2013**, *39*, 1−10.

(4) Restifo, N. P.; Dudley, M. E.; Rosenberg, S. A. Adoptive Immunotherapy for Cancer: Harnessing the T Cell Response. *Nat. Rev. Immunol.* **2012**, *12*, 269−281.

(5) Rosenberg, S. A.; Restifo, N. P. Adoptive Cell Transfer as Personalized Immunotherapy for Human Cancer. *Science* **2015**, *348*, 62−68.

(6) Fesnak, A. D.; June, C. H.; Levine, B. L. Engineered T Cells: The Promise and Challenges of Cancer Immunotherapy. *Nat. Rev. Cancer* **2016**, *16*, 566−581.

(7) Farkona, S.; Diamandis, E. P.; Blasutig, I. M. Cancer Immunotherapy: The Beginning of the End of Cancer. *BMC Med.* **2016**, *14*, 73.

(8) Allison, J. P. Immune Checkpoint Blockade in Cancer Therapy: The 2015 Lasker-Debakey Clinical Medical Research Award. *JAMA, J. Am. Med. Assoc.* **2015**, *314*, 1113−1114.

(9) Sharma, P.; Wagner, K.; Wolchok, J. D.; Allison, J. P. Novel Cancer Immunotherapy Agents With Survival Benefit: Recent Successes and Next Steps. *Nat. Rev. Cancer* **2011**, *11*, 805−812.

(10) Hu, Z.; Ott, P. A.; Wu, C. J. Towards Personalized, Tumour-Specific, Therapeutic Vaccines for Cancer. *Nat. Rev. Immunol.* **2017**, *18*, 168−182.

(11) Azvolinsky, A. Cancer Vaccines: Always a Bridesmaid, Never a Bride. *J. Natl. Cancer Inst.* **2013**, *105*, 248−249.

(12) Bol, K. F.; Schreibelt, G.; Gerritsen, W. R.; de Vries, I. J.; Figdor, C. G. Dendritic Cell-Based Immunotherapy: State of the Art and Beyond. *Clin. Cancer Res.* **2016**, *22*, 1897−1906.

(13) Handy, C. E.; Antonarakis, E. S. Sipuleucel-T for the Treatment of Prostate Cancer: Novel Insights and Future Directions. *Future Oncol.* **2018**, *14*, 907−917.

(14) Türeci, Ö.; Vormehr, M.; Diken, M.; Kreiter, S.; Huber, C.; Sahin, U. Targeting the Heterogeneity of Cancer With Individualized Neoepitope Vaccines. *Clin. Cancer Res.* **2016**, *22*, 1885−1896.

(15) Whiteside, T. L.; Demaria, S.; Rodriguez-Ruiz, M. E.; Zarour, H. M.; Melero, I. Emerging Opportunities and Challenges in Cancer Immunotherapy. *Clin. Cancer Res.* **2016**, *22*, 1845−1855.

(16) Zimmermann, S.; Lepenies, B. Glycans as Vaccine Antigens and Adjuvants: Immunological Considerations. *Methods Mol. Biol.* **2015**, *1331*, 11−26.
(17) Anish, C.; Schumann, B.; Pereira, C. L.; Seeberger, P. H. Chemical Biology Approaches to Designing Defined Carbohydrate Vaccines. *Chem. Biol.* **2014**, *21*, 38−50.
(18) Lockhart, S. Conjugate Vaccines. *Expert Rev. Vaccines* **2003**, *2*, 633−648.
(19) Lindberg, A. A. Glycoprotein Conjugate Vaccines. *Vaccine* **1999**, *17* (Suppl 2), S28−36.
(20) Huang, Y. L.; Wu, C. Y. Carbohydrate-Based Vaccines: Challenges and Opportunities. *Expert Rev. Vaccines* **2010**, *9*, 1257−1274.
(21) Zheng, X. J.; Yang, F.; Zheng, M.; Huo, C. X.; Zhang, Y.; Ye, X. S. Improvement of the Immune Efficacy of Carbohydrate Vaccines By Chemical Modification on the GM3 Antigen. *Org. Biomol. Chem.* **2015**, *13*, 6399−6406.
(22) Ragupathi, G.; Damani, P.; Srivastava, G.; Srivastava, O.; Sucheck, S. J.; Ichikawa, Y.; Livingston, P. O. Synthesis of Sialyl Lewis(a) (Sle (a), Ca19−9) and Construction of an Immunogenic Sle(a) Vaccine. *Cancer Immunol. Immunother.* **2009**, *58*, 1397−1405.
(23) Son, H. Y.; Apostolopoulos, V.; Kim, C. W. T/Tn Immunotherapy Avoiding Immune Deviation. *Int. J. Immunopathol. Pharmacol.* **2016**, *29*, 812−817.
(24) Brooks, S. A.; Carter, T. M.; Royle, L.; Harvey, D. J.; Fry, S. A.; Kinch, C.; Dwek, R. A.; Rudd, P. M. Altered Glycosylation of Proteins in Cancer: What is the Potential for New Anti-Tumour Strategies. *Anti-Cancer Agents Med. Chem.* **2008**, *8*, 2−21.
(25) Dube, D. H.; Bertozzi, C. R. Glycans in Cancer and Inflammation–potential for Therapeutics and Diagnostics. *Nat. Rev. Drug Discovery* **2005**, *4*, 477−488.
(26) Kobata, A.; Amano, J. Altered Glycosylation of Proteins Produced By Malignant Cells, and Application for the Diagnosis and Immunotherapy of Tumours. *Immunol. Cell Biol.* **2005**, *83*, 429−439.
(27) Kim, Y. J.; Varki, A. Perspectives on the Significance of Altered Glycosylation of Glycoproteins in Cancer. *Glycoconjugate J.* **1997**, *14*, 569−576.
(28) Padler-Karavani, V. Aiming At the Sweet Side of Cancer: Aberrant Glycosylation as Possible Target for Personalized-Medicine. *Cancer Lett.* **2014**, *352*, 102−112.
(29) Angata, T.; Varki, A. Chemical Diversity in the Sialic Acids and Related Alpha-Keto Acids: An Evolutionary Perspective. *Chem. Rev.* **2002**, *102*, 439−469.
(30) Chou, H. H.; Takematsu, H.; Diaz, S.; Iber, J.; Nickerson, E.; Wright, K. L.; Muchmore, E. A.; Nelson, D. L.; Warren, S. T.; Varki, A. A Mutation in Human Cmp-Sialic Acid Hydroxylase Occurred After the Homo-Pan Divergence. *Proc. Natl. Acad. Sci. U. S. A.* **1998**, *95*, 11751−11756.
(31) Tangvoranuntakul, P.; Gagneux, P.; Diaz, S.; Bardor, M.; Varki, N.; Varki, A.; Muchmore, E. Human Uptake and Incorporation of an Immunogenic Nonhuman Dietary Sialic Acid. *Proc. Natl. Acad. Sci. U. S. A.* **2003**, *100*, 12045−12050.
(32) Bardor, M.; Nguyen, D. H.; Diaz, S.; Varki, A. Mechanism of Uptake and Incorporation of the Non-Human Sialic Acid N-Glycolylneuraminic Acid Into Human Cells. *J. Biol. Chem.* **2005**, *280*, 4228−4237.
(33) Padler-Karavani, V.; Yu, H.; Cao, H.; Chokhawala, H.; Karp, F.; Varki, N.; Chen, X.; Varki, A. Diversity in Specificity, Abundance, and Composition of Anti-Neu5Gc Antibodies in Normal Humans: Potential Implications for Disease. *Glycobiology* **2008**, *18*, 818−830.
(34) Padler-Karavani, V.; Hurtado-Ziola, N.; Pu, M.; Yu, H.; Huang, S.; Muthana, S.; Chokhawala, H. A.; Cao, H.; Secrest, P.; Friedmann-Morvinski, D.; Singer, O.; Ghaderi, D.; Verma, I. M.; Liu, Y. T.; Messer, K.; Chen, X.; Varki, A.; Schwab, R. Human Xeno-Autoantibodies Against a Non-Human Sialic Acid Serve as Novel Serum Biomarkers and Immunotherapeutics in Cancer. *Cancer Res.* **2011**, *71*, 3352−3363.
(35) Pearce, O. M.; Laubli, H.; Verhagen, A.; Secrest, P.; Zhang, J.; Varki, N. M.; Crocker, P. R.; Bui, J. D.; Varki, A. Inverse Hormesis of Cancer Growth Mediated By Narrow Ranges of Tumor-Directed Antibodies. *Proc. Natl. Acad. Sci. U. S. A.* **2014**, *111*, 5998−6003.
(36) Fang, R. H.; Jiang, Y.; Fang, J. C.; Zhang, L. Cell Membrane-Derived Nanomaterials for Biomedical Applications. *Biomaterials* **2017**, *128*, 69−83.
(37) Su, J.; Sun, H.; Meng, Q.; Zhang, P.; Yin, Q.; Li, Y. Enhanced Blood Suspensibility and Laser-Activated Tumor-Specific Drug Release of Theranostic Mesoporous Silica Nanoparticles By Functionalizing With Erythrocyte Membranes. *Theranostics* **2017**, *7*, 523−537.
(38) Luk, B. T.; Fang, R. H.; Hu, C. M.; Copp, J. A.; Thamphiwatana, S.; Dehaini, D.; Gao, W.; Zhang, K.; Li, S.; Zhang, L. Safe and Immunocompatible Nanocarriers Cloaked in RBC Membranes for Drug Delivery to Treat Solid Tumors. *Theranostics* **2016**, *6*, 1004−1011.
(39) Villa, C. H.; Pan, D. C.; Zaitsev, S.; Cines, D. B.; Siegel, D. L.; Muzykantov, V. R. Delivery of Drugs Bound to Erythrocytes: New Avenues for an Old Intravascular Carrier. *Ther. Delivery* **2015**, *6*, 795−826.
(40) Steck, T. L. The Organization of Proteins in the Human Red Blood Cell Membrane. A Review. *J. Cell Biol.* **1974**, *62*, 1−19.
(41) Ganguly, K.; Murciano, J. C.; Westrick, R.; Leferovich, J.; Cines, D. B.; Muzykantov, V. R. The Glycocalyx Protects Erythrocyte-Bound Tissue-Type Plasminogen Activator From Enzymatic Inhibition. *J. Pharmacol. Exp. Ther.* **2007**, *321*, 158−164.
(42) Galili, U. Discovery of the Natural Anti-Gal Antibody and Its Past and Future Relevance to Medicine. *Xenotransplantation* **2013**, *20*, 138−147.
(43) Naso, F.; Stefanelli, U.; Buratto, E.; Lazzari, G.; Perota, A.; Galli, C.; Gandaglia, A. Alpha-Gal Inactivated Heart Valve Bioprostheses Exhibit an Anti-Calcification Propensity Similar to Knockout Tissues. *Tissue Eng., Part A* **2017**, *23*, 1181−1195.
(44) Salama, A.; Mosser, M.; Lévêque, X.; Perota, A.; Judor, J. P.; Danna, C.; Pogu, S.; Mouré, A.; Jégou, D.; Gaide, N.; Abadie, J.; Gauthier, O.; Concordet, J. P.; Le Bas-Bernardet, S.; Riochet, D.; Le Berre, L.; Hervouet, J.; Minault, D.; Weiss, P.; Guicheux, J.; et al. Neu5Gc and α1−3 GAL Xenoantigen Knockout Does Not Affect Glycemia Homeostasis and Insulin Secretion in Pigs. *Diabetes* **2017**, *66*, 987−993.
(45) Leviatan Ben-Arye, S.; Yu, H.; Chen, X.; Padler-Karavani, V. Profiling Anti-Neu5Gc IgG in Human Sera With a Sialoglycan Microarray Assay. *J. Visualized Exp.* **2017**, DOI: 10.3791/56094.
(46) Diaz, S. L.; Padler-Karavani, V.; Ghaderi, D.; Hurtado-Ziola, N.; Yu, H.; Chen, X.; Brinkman-Van der Linden, E. C.; Varki, A.; Varki, N. M. Sensitive and Specific Detection of the Non-Human Sialic Acid N-Glycolylneuraminic Acid in Human Tissues and Biotherapeutic Products. *PLoS One* **2009**, *4*, No. e4241.
(47) Padler-Karavani, V.; Song, X.; Yu, H.; Hurtado-Ziola, N.; Huang, S.; Muthana, S.; Chokhawala, H. A.; Cheng, J.; Verhagen, A.; Langereis, M. A.; Kleene, R.; Schachner, M.; de Groot, R. J.; Lasanajak, Y.; Matsuda, H.; Schwab, R.; Chen, X.; Smith, D. F.; Cummings, R. D.; Varki, A. Cross-Comparison of Protein Recognition of Sialic Acid Diversity on Two Novel Sialoglycan Microarrays. *J. Biol. Chem.* **2012**, *287*, 22593−22608.
(48) Siegrist, C.-A. Vaccine Immunology. *Vaccines* **2008**, *5*, 17−36.
(49) Schunk, M. K.; Macallum, G. E. Applications and Optimization of Immunization Procedures. *ILAR J.* **2005**, *46*, 241−257.
(50) Pearce, O. M.; Laubli, H.; Bui, J.; Varki, A. Hormesis in Cancer Immunology: Does the Quantity of an Immune Reactant Matter? *Oncoimmunology* **2014**, *3*, No. e29312.
(51) Okerblom, J.; Varki, A. Biochemical, Cellular, Physiological, and Pathological Consequences of Human Loss of N-Glycolylneuraminic Acid. *ChemBioChem* **2017**, *18*, 1155−1171.
(52) Hedlund, M.; Padler-Karavani, V.; Varki, N. M.; Varki, A. Evidence for a Human-Specific Mechanism for Diet and Antibody-Mediated Inflammation in Carcinoma Progression. *Proc. Natl. Acad. Sci. U. S. A.* **2008**, *105*, 18936−18941.
(53) Samraj, A. N.; Pearce, O. M.; Läubli, H.; Crittenden, A. N.; Bergfeld, A. K.; Banda, K.; Gregg, C. J.; Bingman, A. E.; Secrest, P.;

DOI: 10.1021/acsnano.8b07241
ACS Nano 2019, 13, 2936−2947

Diaz, S. L.; Varki, N. M.; Varki, A. A Red Meat-Derived Glycan Promotes Inflammation and Cancer Progression. *Proc. Natl. Acad. Sci. U. S. A.* **2015**, *112*, 542−547.
(54) Samraj, A. N.; Bertrand, K. A.; Luben, R.; Khedri, Z.; Yu, H.; Nguyen, D.; Gregg, C. J.; Diaz, S. L.; Sawyer, S.; Chen, X.; Eliassen, H.; Padler-Karavani, V.; Wu, K.; Khaw, K. T.; Willett, W.; Varki, A. Polyclonal Human Antibodies Against Glycans Bearing Red Meat-Derived Non-Human Sialic Acid N-Glycolylneuraminic Acid Are Stable, Reproducible, Complex and Vary Between Individuals: Total Antibody Levels Are Associated With Colorectal Cancer Risk. *PLoS One* **2018**, *13*, No. e0197464.
(55) Amon, R.; Ben-Arye, S. L.; Engler, L.; Yu, H.; Lim, N.; Le Berre, L.; Harris, K. M.; Ehlers, M. R.; Gitelman, S. E.; Chen, X.; Soulillou, J. P.; Padler-Karavani, V. Glycan Microarray Reveal Induced Iggs Repertoire Shift Against a Dietary Carbohydrate in Response to Rabbit Anti-Human Thymocyte Therapy. *Oncotarget* **2017**, *8*, 112236−112244.
(56) Yin, J.; Hashimoto, A.; Izawa, M.; Miyazaki, K.; Chen, G. Y.; Takematsu, H.; Kozutsumi, Y.; Suzuki, A.; Furuhata, K.; Cheng, F. L.; Lin, C. H.; Sato, C.; Kitajima, K.; Kannagi, R. Hypoxic Culture Induces Expression of Sialin, a Sialic Acid Transporter, and Cancer-Associated Gangliosides Containing Non-Human Sialic Acid on Human Cancer Cells. *Cancer Res.* **2006**, *66*, 2937−2945.
(57) Scott, A. M.; Wolchok, J. D.; Old, L. J. Antibody Therapy of Cancer. *Nat. Rev. Cancer* **2012**, *12*, 278−287.
(58) Scott, A. M.; Allison, J. P.; Wolchok, J. D. Monoclonal Antibodies in Cancer Therapy. *Cancer Immunity* **2012**, *12*, 14.
(59) Poland, G. A.; Ovsyannikova, I. G.; Jacobson, R. M.; Smith, D. I. Heterogeneity in Vaccine Immune Response: The Role of Immunogenetics and the Emerging Field of Vaccinomics. *Clin. Pharmacol. Ther.* **2007**, *82*, 653−664.
(60) Antia, A.; Ahmed, H.; Handel, A.; Carlson, N. E.; Amanna, I. J.; Antia, R.; Slifka, M. Heterogeneity and Longevity of Antibody Memory to Viruses and Vaccines. *PLoS Biol.* **2018**, *16*, No. e2006601.
(61) Ye, Z.; Qian, Q.; Jin, H.; Qian, Q. Cancer Vaccine: Learning Lessons From Immune Checkpoint Inhibitors. *J. Cancer* **2018**, *9*, 263−268.
(62) Lollini, P. L.; Cavallo, F.; Nanni, P.; Forni, G. Vaccines for Tumour Prevention. *Nat. Rev. Cancer* **2006**, *6*, 204−216.
(63) Bethune, M. T.; Joglekar, A. V. Personalized T Cell-Mediated Cancer Immunotherapy: Progress and Challenges. *Curr. Opin. Biotechnol.* **2017**, *48*, 142−152.
(64) Finn, O. J. Human Tumor Antigens Yesterday, Today, and Tomorrow. *Cancer Immunol. Res.* **2017**, *5*, 347−354.
(65) Padler-Karavani, V. Glycan Microarray Reveal the Sweet Side of Cancer Vaccines. *Cell Chem. Biol.* **2016**, *23*, 1446−1447.
(66) Amon, R.; Reuven, E. M.; Leviatan Ben-Arye, S.; Padler-Karavani, V. Glycans in Immune Recognition and Response. *Carbohydr. Res.* **2014**, *389*, 115−122.
(67) Samraj, A. N.; Läubli, H.; Varki, N.; Varki, A. Involvement of a Non-Human Sialic Acid in Human Cancer. *Front. Oncol.* **2014**, *4*, 33.
(68) Magnani, M.; Chiarantini, L.; Vittoria, E.; Mancini, U.; Rossi, L.; Fazi, A. Red Blood Cells as an Antigen-Delivery System. *Biotechnol. Appl. Biochem.* **1992**, *16*, 188−194.
(69) Banz, A.; Cremel, M.; Mouvant, A.; Guerin, N.; Horand, F.; Godfrin, Y. Tumor Growth Control Using Red Blood Cells as the Antigen Delivery System and Poly(I:C). *J. Immunother.* **2012**, *35*, 409−417.
(70) Banz, A.; Cremel, M.; Rembert, A.; Godfrin, Y. *In Situ* Targeting of Dendritic Cells By Antigen-Loaded Red Blood Cells: A Novel Approach to Cancer Immunotherapy. *Vaccine* **2010**, *28*, 2965−2972.
(71) Springer, G. F. Immunoreactive T and Tn Epitopes in Cancer Diagnosis, Prognosis, and Immunotherapy. *J. Mol. Med. (Heidelberg, Ger.)* **1997**, *75*, 594−602.
(72) Muzykantov, V. R. Drug Delivery By Red Blood Cells: Vascular Carriers Designed By Mother Nature. *Expert Opin. Drug Delivery* **2010**, *7*, 403−427.
(73) Rao, L.; Bu, L. L.; Xu, J. H.; Cai, B.; Yu, G. T.; Yu, X.; He, Z.; Huang, Q.; Li, A.; Guo, S. S.; Zhang, W. F.; Liu, W.; Sun, Z. J.; Wang, H.; Wang, T. H.; Zhao, X. Z. Red Blood Cell Membrane as a Biomimetic Nanocoating for Prolonged Circulation Time and Reduced Accelerated Blood Clearance. *Small* **2015**, *11*, 6225−6236.
(74) Xia, L.; Schrump, D. S.; Gildersleeve, J. C. Whole-Cell Cancer Vaccines Induce Large Antibody Responses to Carbohydrates and Glycoproteins. *Cell Chem. Biol.* **2016**, *23*, 1515−1525.
(75) Schumann, B.; Reppe, K.; Kaplonek, P.; Wahlbrink, A.; Anish, C.; Witzenrath, M.; Pereira, C. L.; Seeberger, P. H. Development of an Efficacious, Semisynthetic Glycoconjugate Vaccine Candidate Against. *ACS Cent. Sci.* **2018**, *4*, 357−361.
(76) Geissner, A.; Seeberger, P. H. Glycan Arrays: From Basic Biochemical Research to Bioanalytical and Biomedical Applications. *Annu. Rev. Anal. Chem.* **2016**, *9*, 223−247.
(77) Pappalardo, F.; Pennisi, M.; Castiglione, F.; Motta, S. Vaccine Protocols Optimization: *In Silico* Experiences. *Biotechnol. Adv.* **2010**, *28*, 82−93.
(78) Zahm, C. D.; Colluru, V. T.; McNeel, D. G. Vaccination With High-Affinity Epitopes Impairs Antitumor Efficacy By Increasing PD-1 Expression on CD8. *Cancer Immunol. Res.* **2017**, *5*, 630−641.
(79) Butterfield, L. H. Cancer Vaccines. *BMJ.* **2015**, *350*, h988.
(80) Zeng, M.; Nourishirazi, E.; Guinet, E.; Nouri-Shirazi, M. The Genetic Background Influences the Cellular and Humoral Immune Responses to Vaccines. *Clin. Exp. Immunol.* **2016**, *186*, 190−204.
(81) Borsig, L.; Wong, R.; Hynes, R. O.; Varki, N. M.; Varki, A. Synergistic Effects of L- and P-Selectin in Facilitating Tumor Metastasis Can Involve Non-Mucin Ligands and Implicate Leukocytes as Enhancers of Metastasis. *Proc. Natl. Acad. Sci. U. S. A.* **2002**, *99*, 2193−2198.

DOI: 10.1021/acsnano.8b07241
ACS Nano 2019, 13, 2936−2947